Morris GE (Orcid ID: 0000-0003-4054-6959)
Kostogrys RB (Orcid ID: 0000-0002-7972-7522)
Rainbow RD (Orcid ID: 0000-0002-0532-1992)

SVEP1 regulates GPCR-mediated vasoconstriction via integrin α9β1 and α4β1

Morris GE[1*], Denniff MJ[1], Karamanavi E[1], Andrews SA[1], Kostogrys RB[2], Bountziouka V[1], Ghaderi-Najafabadi M[1], Shamkhi N[1], McConnell G[1], Kaiser MA[1], Carleton L[3], Schofield C[3], Kessler T[4,5], Rainbow RD[6], Samani, NJ[1], Webb TR[1].

Author Affiliation and email address:

1 Department of Cardiovascular Sciences, University of Leicester and National Institute for Health Research Leicester Biomedical Research Centre, Glenfield Hospital, Leicester, LE3 9QP, United Kingdom.

2 Department of Human Nutrition, Faculty of Food Technology, University of Agriculture in Krakow, Poland (R.B.K.).

3 Horizon Discovery Ltd., 8100 Cambridge Research Park, Cambridge, CB25 9TL, United Kingdom.

4 Department of Cardiology, German Heart Centre Munich, Technical University of Munich, Munich, Germany.

5 German Centre of Cardiovascular Research (DZHK e. V.), Partner Site Munich Heart Alliance, Munich, Germany.

6 Department of Cardiovascular and Metabolic Medicine & Liverpool Centre for Cardiovascular Science, University of Liverpool, Liverpool, L69 3GE.

Morris GE: gem8@leicester.ac.uk, Denniff MJ: md123@leicester.ac.uk, Karamanavi E: eliskaram@gmail.com, Andrews SA: sa619@leicester.ac.uk,

Kostogrys RB: rkostogrys@gmail.com, Bountziouka V: vb134@leicester.ac.uk,

Ghaderi-Najafabadi M: mg874@cam.ac.uk,

Shamkhi N: noor.shamkhi@bioch.ox.ac.uk,

This article has been accepted for publication and undergone full peer review but has not been through the copyediting, typesetting, pagination and proofreading process which may lead to differences between this version and the Version of Record. Please cite this article as doi: 10.1111/bph.15921

McConnell G: gm307@leicester.ac.uk, Kaiser MA: zc3hc1@gmail.com

Carleton L: laura.carleton@horizondiscovery.com,

Schofield C: christine.schofield@horizondiscovery.com,

Kessler T: thorsten.kessler@tum.de, Rainbow RD: richard.rainbow@liverpool.ac.uk,

Samani NJ: njs@leicester.ac.uk, Webb TR: trw126@leicester.ac.uk.

*** Corresponding Author:** Gavin Morris, email: gem8@leicester.ac.uk, telephone: +44(0)116 2044763, address: Department of Cardiovascular Sciences, University of Leicester and National Institute for Health Research Leicester Biomedical Research Centre, Glenfield Hospital, Leicester, LE3 9QP, United Kingdom. ORCID: 0000-0003-4054-6959.

ABSTRACT

Background and purpose

Vascular tone is regulated by the relative contractile state of vascular smooth muscle cells (VSMCs). Several integrins directly modulate VSMC contraction by regulating calcium influx through L-type voltage-gated Ca^{2+} channels (VGCCs). Genetic variants in *ITGA9*, which encodes the α9 subunit of integrin α9β1, and *SVEP1*, a ligand for integrin α9β1, associate with elevated blood pressure, however, neither SVEP1 nor integrin α9β1 have reported roles in vasoregulation. We determined whether SVEP1 and integrin α9β1 can regulate VSMC contraction.

Experimental Approach

SVEP1 and integrin binding were confirmed by immunoprecipitation and cell binding assays. Human induced pluripotent stem cell-derived VSMCs were used in *in vitro* $[Ca^{2+}]_i$ studies, and aortas from a *Svep1*$^{+/-}$ knockout mouse model were used in wire myography to measure vessel contraction.

Key Results

We confirmed the ligation of SVEP1 to integrin α9β1 and additionally found SVEP1 to directly bind to integrin α4β1. Inhibition of SVEP1, integrin α4β1 or α9β1 significantly enhanced $[Ca^{2+}]_i$ release in isolated VSMCs to $G\alpha_{q/11}$-vasoconstrictors. This response was confirmed in whole vessels where a greater contraction to U46619 was seen in vessels from *Svep1*$^{+/-}$ mice compared to littermate controls or when integrin α4β1 or

α9β1 were inhibited. Inhibition studies suggested that this effect was mediated via VGCCs, PKC and Rho A/Rho kinase dependent mechanisms.

Conclusions and Implications

Our studies reveal a novel role for SVEP1 and the integrins α4β1 and α9β1 in reducing VSMC contractility. This could provide an explanation for the genetic associations with blood pressure risk at the *SVEP1 and ITGA9* loci.

Word count: 250

Keywords

SVEP1, integrin α4β1, integrin α9β1, blood pressure, vasoconstriction.

What is already known

- Genetic variants in *SVEP1* associate with elevated blood pressure.

What this study adds

- SVEP1 is a new regulator of vasoconstriction.

Clinical significance

- SVEP1 is a potential therapeutic candidate in vascular hypertension.
- Activation of integrin α9β1 could provide a new treatment in vascular hypertension.

Non-standard Abbreviations

ADAM	a disintegrin and metalloproteinase with thrombospondin motifs
ADAMTS-7	ADAM Metallopeptidase With Thrombospondin Type 1 Motif 7
bFGF	basic fibroblast growth factor
BSA	bovine serum albumin
BOP	*N*-(Benzenesulfonyl)-L-prolyl-L-*O*-(1-pyrrolidinylcarbonyl)tyrosine
Ca^{2+}	calcium ion
CAD	coronary artery disease
CAEC	coronary artery endothelial cell
Cch	carbachol
CCP	complement control protein
c-SRC	proto-oncogene tyrosine-protein kinase Src
CRISPR	clustered regularly interspaced short palindromic repeats
EC	endothelial cell
ECM	extracellular matrix
EGF	epidermal growth factor
ET-1	endothelin-1
GFP	green fluorescent protein
GFR	growth factor reduced
GPCR	G protein coupled receptor
HEK	human embryonic kidney
HUVEC	human umbilical vein endothelial cell
IF	immunofluorescence
IHC	immunohistochemistry
IP	immunoprecipitation
IP3	inositol 1,4,5-trisphosphate
iPSC	induced pluripotent stem cell
KO	knockout
MBP	mannose binding protein
MLCK	myosin light chain kinase

MLCP	myosin light chain phosphatase
NTC	non-targeting control
PDGF	platelet-derived growth factor
PIP2	phosphatidylinositol 4,5-bisphosphate
PKC	protein kinase C
PLC	phospholipase C
PE	phenylephrine
ROCK	Rho A/Rho kinase
SD	standard deviation
siRNA	small interfering RNA
SVEP1	Sushi, von Willebrand factor type A, EGF and pentraxin domain-containing protein 1
TGF	transforming growth factor
UTP	uridine-5'-triphosphate
VGCC	L-type voltage-gated calcium channel
VSMC	vascular smooth muscle cell
WT	wild-type

1. INTRODUCTION

Arterial diseases including hypertension and coronary artery disease (CAD) display a degree of dysregulation in the contractile behaviour of the smooth muscle. Vascular tone is regulated by the relative contractile state of vascular smooth muscle cells (VSMCs) (Brozovich, Nicholson, Degen, Gao, Aggarwal & Morgan, 2016; Webb, 2003). VSMC contraction provides force generation through the phosphorylation of myosin light chain kinase (MLCK) which facilitates interaction between actin and myosin filaments. MLCK is directly phosphorylated by calcium-bound calmodulin. Increases in intracellular calcium concentrations ($[Ca^{2+}]_i$) occur via activation of $G_{\alpha q}$-Protein Coupled Receptors (GPCRs) leading to PLCβ-mediated Ca^{2+} ion release from the sarcoplasmic reticulum, and PKC-mediated activation of L-type voltage-gated calcium channels (VGCCs) leading to an influx of extracellular Ca^{2+} ions, with the calmodulin-dependent MLCK contraction initiated by this elevation in $[Ca^{2+}]_i$. In addition to activation of MLCK, inhibition of myosin light chain phosphatase (MLCP), via PKC and the RhoA/Rho kinase (ROCK) pathways (Touyz et al., 2018), enables the light chain of myosin to remain phosphorylated and thus prolong contraction. Whilst these central signalling pathways controlling contraction are widely characterised (Brozovich, Nicholson, Degen, Gao, Aggarwal & Morgan, 2016; Touyz et al., 2018; Webb, 2003), modulation of these pathways remains ill-defined.

Several integrins can directly modulate vascular smooth muscle cell contraction by regulating calcium influx through VGCCs (Mogford, Davis & Meininger, 1997; Mogford, Davis, Platts & Meininger, 1996; Waitkus-Edwards et al., 2002; Wu, Davis, Meininger, Wilson & Davis, 2001; Wu, Mogford, Platts, Davis, Meininger & Davis, 1998). Within the airway, integrin α9β1 has been specifically identified as preventing exaggerated airway smooth muscle contraction, where conditional knockout of the α9 subunit in airway smooth muscle causes a spontaneous increase in pulmonary resistance in response to multiple GPCR agonists (Chen et al., 2012). Sushi, von Willebrand factor type A, EGF and pentraxin domain-containing protein 1 (SVEP1), a high affinity ligand for integrin α9β1 (Sato-Nishiuchi et al., 2012), is a 390 kDa secreted extracellular matrix (ECM) protein comprised of sushi (complement control protein (CCP)), von Willebrand factor type A, epidermal growth factor-like, and pentraxin domains (Shur, Socher, Hameiri, Fried & Benayahu, 2006). SVEP1 is a cell adhesion molecule (Gilges

et al., 2000; Sato-Nishiuchi et al., 2012; Schwanzer-Pfeiffer, Rossmanith, Schildberger & Falkenhagen, 2010; Shur, Socher, Hameiri, Fried & Benayahu, 2006) required for normal development of lymphatic vessels (Karpanen et al., 2017; Morooka et al., 2017) and epidermal differentation (Samuelov et al., 2017). A low frequency coding variant rs111245230 (p.D2702G) within SVEP1 associates with elevated blood pressure (BP) (Myocardial Infarction et al., 2016) and CAD (Myocardial Infarction Genetics, 2016). rs111245230 is situated adjacent to the binding motif through which SVEP1 binds to integrin α9β1. Genetic variants associated with reduced expression of *ITGA9*, which encodes the α9 subunit of integrin α9β1, have also been reported to associate with increased BP (Evangelou et al., 2018; Levy et al., 2009). Neither SVEP1 nor integrin α9β1 have a reported role in vasoregulation, however direct activation of integrin α4β1, with which integrin α9β1 forms an integrin subfamily (Palmer, Ruegg, Ferrando, Pytela & Sheppard, 1993), can induce VSMC contraction (Waitkus-Edwards et al., 2002). Recently, two studies investigated the effect of *Svep1* deficiency in relation to the development of atherosclerosis in mice (Jung et al., 2021; Winkler et al., 2020). Notably, these studies, which utilised similar mouse models, detected contrary effects of *Svep1* deficiency with one reporting a reduction in atherosclerosis (Jung et al., 2021) and the other identifying an increase in plaque size (Winkler et al., 2020). The reason for this difference in phenotype is currently unclear. Neither study explored SVEP1 in relation to BP or smooth muscle contraction.

Due to the genetic association between variants in *SVEP1* and *ITGA9* with BP, the described roles for integrins in smooth muscle vasoregulation, including integrin α9β1 in airway smooth muscle, we hypothesised that SVEP1 and integrin α9β1 could regulate vascular smooth muscle contractility. Therefore, in the present study we analysed the effect of SVEP1 and integrin α9β1 inhibition upon $G_{\alpha q}$PRC-mediated VSMC contraction in isolated VSMCs and whole blood vessels.

2. Methods

2.1 Cell culture

All cell lines were maintained at 37 °C in a 5% CO_2 incubator. HEK293 wild type cells were maintained in DMEM supplemented with 10% (*v/v*) foetal calf serum (FCS) and

integrin α4 over-expressing cells were maintained in DMEM supplemented with 10% (*v/v*) FCS and 500 μg mL^{-1} geneticin.

Human induced pluripotent stem cells (iPSCs) (Cell line GM23720, NIGMS collection from the Coriell institute for medical research) were maintained on growth factor reduced (GFR) matrigel-coated plates in mTeSR™ Plus media (STEMCELL Technologies). Cells were passaged using ReLeSR™ (STEMCELL Technologies) and re-plated as small clumps of cells at a dilution of 1:10 to 1:20. For SMC differentiation, iPSCs were dissociated with Accutase and plated on GFR Matrigel at a density of $2.5x10^4$ cells cm^{-2} in ROCK inhibitor (Y-27632, 10 μM)-supplemented mTeSR™ Plus media for 24 hours. Media was replaced with STEMdiff™ MIM (STEMCELL Technologies) for 72 hours, with media replaced every 24 hours. After 72 hours, the MIM was replaced with SMC Induction medium consisting of STEMdiff™ APEL-2 medium (STEMCELL Technologies) supplemented with 50 ng ml^{-1} VEGF and 25 ng ml^{-1} BMP4 for 4 days, with media replaced after 2 days. On day 8, cells were dissociated using Accutase and plated on collagen IV (30 μg ml^{-1} coated wells) in Smooth Muscle Cell Growth Medium 2 (SMGM2 (Promocell) supplemented with 10 ng ml^{-1} PDGF-BB, 2 ng ml^{-1} TGFβ, 0.5 ng ml^{-1} EGF, 2 ng ml^{-1} bFGF, 5 μg/ml^{-1} insulin and 0.05 ml/ml FCS for a further 14 days. Experimentation was conducted on cells between day 32 and day 40.

2.2 Generation of SVEP1$^{-/-}$ iPSC lines

An isogenic pair of *SVEP1* GM23720 iPSC line was generated by CRISPR genome editing in collaboration with Horizon Discovery Ltd. A guide RNA targeting GAGACCGCGCCCGGGGCCC*CCGGGAGTATCCCCGCGCCG*CCCGCTCCTGGC GA, a region within exon 1 of Ensembl SVEP1 transcript SVEP1-003 (ENST00000374469.5) was designed. The underlined highlighted sequence indicates the protospacer adjacent motif and the italic sequence indicates the guide RNA. This guide RNA was co-transfected into iPSCs with a plasmid expressing CAS9. After transfection, iPSCs were serially diluted into 96 well plates to generate single cell clones. Single cell clones were genotyped by sequencing PCR products generated using primers CAGCCGCTCTGTCTCCAG and AGGAGATGGCAGGGATCTCT.

2.3 Cell transfection

iVSMCs were transiently transfected with non-targeting control (Qiagen siRNA, cat: 1022076), ITGA9 (Qiagen FlexiTube siRNA, cat: S100034272), SVEP1 (ThermoFisher Scientific Stealth siRNA, cat: 1299001) or ITGA4 (Dharmacon SMARTpool of 4 siRNAs, cat: SO-2757075G) (all 100 nM) using Lipofectamine RNAiMAX (ThermoFisher) diluted in OptiMEM in SMGM2. Media was changed after 24 hours, with cells used at 48 hours.

2.4 Single-Cell Ca^{2+} iVSMC Imaging

iVSMCs were loaded with the Ca^{2+}-sensitive dye Fluo-3, AM (3 µM, 60 min) (ThermoFisher). Cells were maintained at 37°C using a Peltier unit and continually perfused with Krebs-Henseleit buffer (mM: 134 NaCl, 6 KCl, 1 $MgCl_2$, 1.2 KH_2PO_4, 10 glucose, 10 HEPES, 1.3 $CaCl_2$, pH 7.4). Real-time images were taken using an epifluorescence Nikon Eclipse TE200 microscope (Nikon) (×20 objective) and Volocity 6.1.1 image software (Quorum Technologies). For extracellular Ca^{2+} depletion studies, 10 mM EGTA was added, and $CaCl_2$ was removed from the Krebs-Henseleit buffer, with cells perfused in this buffer for 2 minutes prior to stimulation. For pharmacological inhibition studies, BOP (*N*-(Benzenesulfonyl)-L-prolyl-L-*O*-(1-pyrrolidinylcarbonyl)tyrosine) (3 µM) or Y-27632 (10 µM) were added to the cell coverslips 30 minutes prior to stimulation. Cells were stimulated with vasoconstrictors applied via the perfusion line for 45 seconds, and Fluo-3 emission was assessed at ≥520 nm. The maximal fluorescent emission in cells that responded to vasoconstrictor application was measured and then averaged per coverslip to provide a single independent value. $[Ca^{2+}]_i$ changes are displayed as the fold mean of the fluorescence emission relative to basal fluorescence (F/F_0), assigning a value of 0 to F_0, to control for sources of variation of baseline fluorescence.

2.5 Mouse Studies

Animal experimentation was approved by the local animal ethics committee and performed according to ARRIVE (Animal Research: Reporting of In Vivo Experiments) guidelines (Percie du Sert et al., 2020), and the recommendations made by the *British Journal of Pharmacology* (Lilley et al., 2020), under United Kingdom Home Office Project Licence (P4E9A1CCA). All mice were housed in a specific pathogen-free facility in an individually ventilated caging system. Mice were group housed wherever

possible, and their health status was checked routinely. No mice demonstrated any adverse effects. C57BL/6J mice were purchased originally from Charles River, then bred in the Preclinical Research Facility in the University of Leicester, to provide animals for the study. Genetically altered animals, B6N(Cg)-Svep1tm1b(EUCOMM)Hmgu/J (reporter-tagged deletion allele, *Svep1*$^{+/-}$) was purchased from the Jackson Laboratory (Bar Harbor, ME, USA). In accordance with Schedule 1 of the Animals (Scientific Procedures) Act 1986 (U.K.), 13-24 week-old mice of both genders were euthanised by dislocation of the neck before aortas were harvested and used in wire myography experiments.

2.6 Wire myography

Aortic ring segments of ~2 mm in length were prepared using a dissecting microscope. Aortic rings where integrin α4 and/or α9 were inhibited were incubated with either BOP or blocking antibodies overnight at 37 °C in a 5% CO_2 incubator in DMEM basal media. Aortic rings were mounted on 2 intra-luminal steel wires in a 4-channel Mulvany-Halpern wire myograph (Danish Myo Technology). Vessels were bathed in a HEPES buffered bath solution containing (mM): NaCl 136, KCl 5, $MgSO_4$ 1.2, $CaCl_2$ 1.8, glucose 5, mannitol 15, HEPES 10, NaH_2PO_4 0.5, Na_2HPO_4 0.5 pH 7.4. Isometric tension was continuously recorded using a Powerlab 16/35 AD converter and the LabChart software (LabChart v5, ADInstruments, UK). Vessels were equilibrated, and an optimum static tension of 1.2 mN was observed for a period of at least 50 minutes before NaCl was reduced to 81 mM and replaced with 60 mM KCl solution for 10 minutes, every 10 minutes for three rounds of high K^+ solution application to test vascular function. Any vessels that contracted with an amplitude less than 2 mN were discounted from the studies. A single dose of pharmacological inhibitors (nifedipine (3 µM), BIM (I) (10 µM), BOP (3 µM), or Y-27632 (10 µM) were added directly to the organ bath, maintained at 37°C, 30 minutes prior to addition of cumulative concentrations of the vasoconstrictors (U46619: 1 - 100 nM, PE 0.5 – 200 µM), all vasoconstrictors were added at 10-minute intervals). Aortic rings from the same animals were used for treatment and control experiments. For all experiments, data was expressed as the maximum tension (mN/mm) generated. Due to genotype requirements, randomisation between groups was not performed when using tissue from *Svep1*$^{+/-}$ and comparing to wild-type littermates. Analysis was performed semi-blinded to treatment and genotype by an independent analyst.

2.7 RNA extraction, cDNA synthesis and RT-qPCR

Total RNA was extracted with RLT buffer and purified using an RNeasy mini kit (Qiagen®) according to manufacturer's instructions. RNA yield was determined using a NanoDrop ND-8000 spectrometer. Genomic DNA was removed by DNase I incubation using the RNase-Free DNase Set (Qiagen®) and RNA was converted to cDNA using SensiFAST cDNA synthesis kit (Geneflow). Quantitative reverse transcription PCR (RT-qPCR) was performed using SYBR® 3 Green master mix with amplification carried out in triplicate using a Rotor-Gene® Q (Qiagen®) with each triplicate providing one independent value. Expression levels were calculated using relative standard curve methods and normalised to the reference gene *RPLP0* (Akamine et al., 2007). Primer sequences are listed in Table S1.

2.8 Immunohistochemical (IHC) and immunofluorescence (IF) staining

Immunohistochemistry has been conducted to comply with the recommendations made by the *British Journal of Pharmacology* (Alexander et al., 2018). Primary antibodies that were used for IHC and IF are listed in Table S2. Heat- induced antigen retrieval was performed with Antigen Unmasking Solution, Tris-Based (Vector, H-3301) for all antibodies. For IHC staining, endogenous peroxidase activity was blocked in 0.3% H_2O_2 in deionised water. Nonspecific binding was reduced by incubation in 2.5% goat serum. Sections were treated with mouse Ig blocking reagent (Vector, MKB-2213-1) before application of the primary mouse antibody. Rabbit primary antibody binding was detected with goat anti-rabbit ImmPRESS HRP goat anti-rabbit IgG (Vector, MP-741) and mouse primary antibody binding was detected with Mouse-on-Mouse ImmPRESS anti-mouse Ig reagent (Vector, MP-2400). Colour was developed with DAB-substrate chromogen system (Vector, SK-4100). Images were acquired with a DM2500 Leica microscope (Leica Microsystems).

For IF staining of aortic sections, rabbit primary antibody binding was detected with goat anti-rabbit IgG (Alexa Fluor-488), mouse primary antibody binding was detected with goat anti-mouse IgG (Alexa Fluor-647), and goat primary antibody was detected with donkey anti-goat IgG (Alexa Fluor-594). DAPI was used for nuclei visualization. Images were acquired using an Olympus FV1000 confocal laser scanning microscope with images analysed using Fiji (Schindelin et al., 2012).

iVSMCs or HUVECs were grown on µ-Slide 8 well chamber slides (Thistle Scientific) and fixed in 4% PFA. SVEP1, Integrin α4 and α9 staining was performed on non-permeabilised cells. For all other staining, cells were permeabilised in 0.5% Triton-X. Non-specific binding was reduced by incubation in 1% bovine serum albumin (BSA), 22.5 mg ml-1 glycine, 0.1% tween-20 PBS solution, with additional blocking in a 10% goat serum PBS solution. Cells were incubated overnight at 4°C in primary antibody (listed in Table S2) diluted in 10% goat serum. After washing, cells were incubated in 10% goat serum containing complementary secondary antibodies. Nuclei were visualised by DAPI counterstaining. Images were acquired using an Olympus FV1000 confocal laser scanning microscope with images analysed using Fiji (Schindelin et al., 2012).

2.9 Flow cytometry

iVSMCs were dissociated using Accutase. $CD140^{+}$ staining was quantified using single cell suspensions incubated using an APC-direct labelled antibody diluted in flow buffer (BSA (0.5%), EDTA (2 mM), PBS, pH 7.2). Samples were run on a Beckman Coulter Gallios flow cytometer and analysed using Kaluza flow cytometry analysis software (Beckman Coulter).

2.10 Western blotting

Western blotting has been conducted to comply with the recommendations made by the *British Journal of Pharmacology* (Alexander et al., 2018). Cells were lysed in modified RIPA buffer (Tris HCl (50 mM), EDTA (1 mM), Halt Protease Inhibitor cocktail (ThermoFisher), pH7.4. Western Blot Analysis Protein content was measured using the Novex® protein separation kit (ThermoFisher). Equal amounts of protein lysates were separated by SDS-PAGE before blotting onto nitrocellulose membrane. Membranes were blocked in 5% milk powder, probed with primary antibodies (see Table S2) diluted in 5% milk powder, detected with horseradish peroxidase conjugated secondary antibodies diluted in 5% milk powder, and visualised by enhanced chemiluminescence (GE Healthcare). Quantitative signals were derived by densiometric analysis using ImageQuant™ TL on an ImageQuant™ LAS 4000 Luminescent Image Analyzer (Fujifilm). Western blot densitometry values were normalised to the relative quantification of the corresponding intensity of the total

protein, and changes in expression were expressed as the fold mean of control cells assigning a value of 1 to the control.

2.11 Immunoprecipitation

Constructs expressing ITGA9-GFP and SVEP1-FLAG were co-transfected into HEK293A cells and a construct expressing ITGA4 was transfected into HEK293A or HEK293A cells stably overexpressing SVEP1-FLAG using Lipofectamine 2000 (ThermoFisher). 48 hours post transfection the transfected cells were scraped into lysis buffer (mM: 50 Tris-HCL, 150 NaCl, 1 EDTA, 1% Triton-X-100 and 1x phosphatase and protease inhibitors). Lysates were incubated on ice (15 minutes), sonicated, and cleared by centrifugation at 17,000 *g*. Anti-FLAG–agarose beads (Sigma Aldrich) were prepared by washing 3x in wash buffer (mM: 50 Tris-HCL, 150 NaCl and 1 EDTA). Cell lysate was added to the pelleted beads. The IP reactions were incubated for 90 minutes at 4°C with agitation. The pulled down proteins were denatured from the beads using 25 µL of a solution containing 50% 4x lauryl dodecyl sulphate sample buffer, 45% wash buffer, 5% β-mercaptoethanol. The ITGA9-GFP was detected in a western using an anti-GFP antibody. The ITGA4 proteins were detected in a western using an anti-integrin α4 antibody (primary antibodies listed in Table S2). These westerns were repeated a minimum of 5 times.

2.12 Recombinant protein production

Plasmid expressing mannose-binding protein (MBP)-tagged CCP21 or CCP22 domains of SVEP1, or MBP alone under the control of an iso-propyl-thio-β-glactosidase (IPTG) inducible promoter were transformed into E.Coli BCL21 cells. Transformed cells were grown in lysogeny broth (LB) media containing 100 µg mL^{-1} ampicillin to an optical density of between 0.6 and 0.8 at 600 nm. Protein expression was induced by addition of 0.5 mM IPTG. Cell culture was pelleted, lysed and sonicated with the lysate cleared by centrifuging. The MBP-tagged proteins were immunoprecipitated from the cleared cell lysate using amylose beads (New England Biolabs). The protein was eluted from the beads using an affinity purification column with 10 mM maltose in PBS-T. The elution buffer was exchanged using spin columns with a molecular weight cut-off of 30 kDa. Purified protein was run on a 4-12 % Bis tris gel with protein visualised by Coomassie staining.

2.13 Stable cell line generation

To generate integrin-α4 expressing cells, HEK293A cells were transfected with 2 µg ITGA4 or SVEP1-FLAG plasmid using lipofectamine 2000 (ThermoFisher) and selected using 800 µg mL^{-1} geneticin 48 hours post transfection. Cells were diluted to single cell to isolate individual colonies and clones expressing integrin-α4 or SVEP1-FLAG were identified using anti-integrin α4 or anti-FLAG antibody respectively (Table S2). To generate an integrin α9-GFP stable line HEK293A cells were transfected using the NEPA21 Electroporator system (Nepagene). Cells were transfected with 10 µg integrin α9-GFP plasmid in OptimMEM. After 48 hours, cells were selected using 500 µg mL^{-1} geneticin. Cells were diluted to single cell to isolate individual clones, with clones expressing integrin α9-GFP identified by fluorescent microscopy.

2.14 Recombinant protein cell binding assay

100 nM recombinant MBP control, MBP tagged-CCP21 or MBP tagged-CCP22 was coated onto a 96 well tissue culture plate. Non-specific binding was blocked using DMEM containing 10 mg ml^{-1} bovine serum albumin, 10 mM HEPES. 20,000 HEK293 control ($\alpha4/\alpha9^-$), integrin α4β1 ($\alpha4\beta1^+$), or α9β1 overexpressing ($\alpha9\beta1^+$) cells were seeded onto the coated plates in blocking buffer in triplicate with each triplicate providing one independent value. The $\alpha4\beta1^+$ cells were incubated for 3 hours and the $\alpha9\beta1^+$ cells were incubated for 30 mins at 37ºC and incubated at 37ºC for 30 mins. Plates were washed, fixed with 4% PFA and visualised using DAPI. The number of adhered cells was measured using Fiji (Schindelin et al., 2012). The data was normalised as fold mean over cell adherence to MBP control cells, and changes in adherence are expressed as the fold change over MBP control cells, assigning a value of 1 to the control, to adjust for bound cell numbers.

2.15 Data and Statistical Analysis

The data and statistical analysis comply with the recommendations of the *British Journal of Pharmacology* on experimental design and analysis in pharmacology (Curtis et al., 2018). Each group size was the number of independent values, with the exact group size for each experimental group provided in the figure legends. Group size is the number of independent values, with studies designed to generate groups of equal size, however, outliers were excluded from the single-cell Ca^{2+} iVSMC imaging studies and the wire myography studies using pre-defined criteria: In single-

cell imaging, if no cells responded to vasoconstrictor application within a field of view, the value was excluded. In wire myography experiments, contractility was determined by depolarisation in a high K^+ solution, with vessels that contracted with an amplitude less than 2 mN being discounted from the studies.

For figures 1, SF 1 and SF 6, the observational and conformational data were not subjected to statistical analysis owing to their small group size ($n < 5$). Statistical analysis performed only for studies where each group size was more than n=5. To reduce unwanted sources of variation derived from different experimental settings, specific data sets were normalised (cell binding assay, Fig. 1, single cell imaging (Fig. 3&4, SF. 8&9), qPCR (SF. 1&6), and western blotting (SF. 6).

Continuous data were presented as mean ± SD. All data transformations are presented as the fold mean over controls. The independent samples Student's t-test was used to evaluate the differences between two groups. One-way ANOVA was used to evaluate differences among >2 experimental groups. If the overall F-test was statistically significant, and the variance between groups was constant we also performed pairwise comparisons using Tukey's multiple comparisons test. To examine the effect of genotype or the application of a targeted antagonist on U46619 (1-100 nM) mediated contraction we fitted mixed-effects models. We implemented the restriction maximum likelihood estimation, with random intercepts for the different mice, to account for the within-mouse variation. Interactions of the genotype with the different levels of concentration were tested. To decide upon the inclusion of the interaction term we used the Bayesian information criterion (BIC). The interaction term was kept in the model if it produced a smaller BIC value compared to a model with no interaction term. For the models with the interaction term this meant that the genotype effect on vessel tension was not always constant, therefore it varied according to the levels of the U46619 concentration (i.e., dependent of vasoconstrictor concentration: Fig. 5C, 6A, 6B, 6C & 6D). For the models with no interaction term this meant that the genotype effect on vessel tension was independent on the vasoconstrictor concentration (Fig. 5A, 5B, 5D, 6E & SF. 10 E). Point estimates are stated in text, whilst the 95% confidence intervals (95% CI) are plotted in the relevant figures. The models were investigated by inspecting Q-Q plots and histograms to evaluate the assumption of normality. A value of $P<0.05$ was considered statistically significant. All statistical analyses were performed using GraphPad Prism 8.0 (GraphPad Software

Inc., USA, RRID:SCR_002798) or Stata 16 (StataCorp, 2019. Stata Statistical Software: Release 16. College Station, TX: StataCorp LLC.).

2.16 Nomenclature of targets and ligands

Key protein targets and ligands in this article are hyperlinked to entries in http://www.guidetopharmacology.org and are permanently archived in the Concise Guide to PHARMACOLOGY 2021/22 (Alexander et al., 2021a; Alexander et al., 2021b; Alexander et al., 2021c; Alexander et al., 2021d; Alexander et al., 2021e).

3. Results

3.1 SVEP1 binds to integrin α4β1 and α9β1

SVEP1 is a known ligand for integrin α9β1 (Sato-Nishiuchi et al., 2012), but whether SVEP1 can bind to the closely related integrin α4β1 (Palmer, Ruegg, Ferrando, Pytela & Sheppard, 1993) has not been reported. Using immunoprecipitation we found SVEP1 to bind to integrin α4 (Fig. 1A), and confirmed the ligation of SVEP1 to integrin α9 (Fig. 1B). SVEP1 binds to integrin α9β1 through its 21st CCP21 domain (CCP21) (Sato-Nishiuchi et al., 2012). In addition to demonstrating the direct ligation of SVEP1 to integrin α4, we performed exploratory investigations to determine whether SVEP1 interacts with α4 via the same domain as it interacts with integrin α9 using a cell adhesion assay. We coated tissue culture plastic with 100 nM mannose-binding protein (MBP), MBP-tagged CCP21, or CCP22 domain peptides. HEK293 cells overexpressing the integrin α4 subunit bound to the CCP21 peptide greater than either MBP or CCP22 control proteins (Fig. 1C), with similar results seen for HEK293 cells overexpressing the integrin α9 subunit (Fig. 1D).

3.2 SVEP1, integrins α4β1and α9β1 are expressed in vascular smooth muscle

We explored the gene expression of *SVEP1*, *ITGA4* and *ITGA9* in both endothelial cells (ECs) and VSMCs, the primary resident cell types of the blood vessel wall. Each gene was expressed in both cell types with *SVEP1* (SF. 1A) and *ITGA4* (SF. 1B) more highly expressed in VSMCs and *ITGA9* expression higher in ECs (SF. 1C), in keeping with the previous atherosclerosis studies (Jung et al., 2021; Winkler et al., 2020). Subsequent protein analysis revealed expression of SVEP1, integrin α4β1 and integrin α9β1 within the arterial wall, with all three proteins localised to VSMCs within the media layer of the arterial wall (Fig. 2A, 1-3, & SF.2). Immunofluorescent dual staining

showed SVEP1 to be in close proximity with integrin α4β1 (Fig. 2B, 1-3) and integrin α9β1 (Fig. 2B, 4-6) in mouse aorta, and isolated human VSMCs (Fig. 2C, 1-3 & 4-6 respectively). SVEP1 protein was found to be in close proximity to both integrin α4β1 and integrin α9β1 at low levels in isolated HUVEC cells (SF.3). Relevant staining controls are shown in SF4.

3.3 Development of a human VSMC *in vitro* platforms for SVEP1 vasoconstrictive investigations

A limiting factor in smooth muscle contraction experiments is the loss of membrane channels and GPCRs within days of culturing following tissue extraction (Halayko, Salari, Ma & Stephens, 1996; Ihara, Hirano, Hirano, Nishimura, Nawata & Kanaide, 2002; Widdop, Daykin & Hall, 1993). To overcome this issue, we developed a human iPSC-derived vascular smooth muscle cells (iVSMC) model with iPSCs differentiated into a mesodermal phenotype as a monolayer prior to differentiation into specialised VSMC phenotype (Maguire, Xiao & Xu, 2017). iPSC pluripotency gene expression is stopped by day 4 (SF. 5B, 1&5). Cells differentiate into primitive streak cells (days 2-4, SF. 5B, 2&6) and mesodermal progenitors (days 3-6, SF. 5B, 3), with 94% of cells $CD140^{+}$ at day 8 (SF. 5B, 7). After a further 12 days culture in TGFβ and PDGF supplemented media, the iVSMCs express a panel of smooth muscle contractile markers (SF. 5C), reliably physically contract a collagen gel (SF. 5D, 1), and display an increase in $[Ca^{2+}]_i$ in response to a panel of GPCR vasoconstrictors (SF.5D, 2) compared to the limited contractile responses seen in cultured primary human VSMCs (SF. 5D, 3).

To interrogate the role of SVEP1 integrin α4β1 and α9β1 in VSMC contraction we used two complimentary methods. Gene expression of *SVEP1*, *ITGA9* and *ITGA4* were knocked down using siRNA in differentiated iVSMCs. We achieved a knockdown efficiency between 60-90% at the RNA level, with protein knockdown confirmed for integrin α4 and α9 by western blotting and immunofluorescence, and SVEP1 by immunofluorescence alone (SF. 6). We were unable to detect a band of the correct molecular weight to reliably quantify SVEP1 protein expression. In addition to siRNA depletion of *SVEP1*, we generated *SVEP1*$^{-/-}$ knockout iPSCs using CRISPR-Cas9 which contain a 1 base pair deletion at position 130 in the coding sequence within

exon 1 of *SVEP1* (SF.7). This isogenic pair of iPSCs were then differentiated into iVSMCs and used in $[Ca^{2+}]_i$ experiments.

3.4 SVEP1 and integrin α4 or α9 deficiency enhances VSMC $[Ca^{2+}]_i$ elevation

SVEP1 siRNA treated isolated iVSMCs showed significant increases in cytosolic $[Ca^{2+}]_i$ to several vasoconstrictors that signal via different GPCRs including endothelin (ET)-1 (Fig. 3A), carbachol (Fig. 3B), and U46619 (Fig. 3C) compared to non-targeted control (NTC) siRNA transfected cells. This effect was confirmed in *SVEP1*$^{-/-}$ iVSMCs where maximal $[Ca^{2+}]_i$ elevation to ET-1 (SF. 8A) and carbachol (SF. 8B), were also significantly enhanced compared to isotype control iVSMCs. Increases in intracellular Ca^{2+} occur through Ca^{2+} release from the sarcoplasmic reticulum and via an influx of extracellular Ca^{2+} through VGCCs (Brozovich, Nicholson, Degen, Gao, Aggarwal & Morgan, 2016; Nelson & Quayle, 1995; Touyz et al., 2018; Webb, 2003). To investigate the source of the increased $[Ca^{2+}]_i$ extracellular Ca^{2+} was depleted in the imaging buffer, or the VGCC antagonist nifedipine was added prior U46619 application. Both removal of extracellular Ca^{2+} and VGCC blockage minimised $[Ca^{2+}]_i$ accumulation upon U46619 stimulation in both *NTC* and *SVEP1* siRNA treated cells (Fig. 3D), indicating the elevation of $[Ca^{2+}]_i$ was primarily achieved through the influx of extracellular Ca^{2+}. Inhibition of either integrin α4β1 or α9β1 using siRNA caused enhanced iVSMC $[Ca^{2+}]_i$ elevation to ET-1 (Fig. 4A), whilst simultaneous inhibition of integrin α4β1 and α9β1 did not cause any additional $[Ca^{2+}]_i$ increase (Fig. 4A). Similarly, *SVEP1* deficiency and blocking either integrin α4β1 (SF. 9A), integrin α9β1 (SF. 9B), or integrin α4β1 and α9β1 dual inhibition using siRNA (Fig. 4B) or the dual integrin α4β1/α9β1 inhibitor BOP (Pepinsky et al., 2002) (Fig. 4C) did not cause additional ET-1-mediated $[Ca^{2+}]_i$ elevation compared to cells treated with *SVEP1* siRNA alone. Similar results were seen in iVSMCs stimulated with carbachol (SF. 9C) and was confirmed in ET-1-stimulated *SVEP1*$^{-/-}$ iVSMCs treated with BOP (SF. 9D). These data show that SVEP1 reduces iVSMC Ca^{2+} release to several $G_{\alpha q/11}$ agonists via integrin α4β1 and α9β1.

3.5 SVEP1-integrin α4/9 signalling inhibits whole vessel contraction

Perinatal mortality is observed in *Svep1* null mice, with mice displaying edema at E18.5 (Morooka et al., 2017). *Svep1*$^{+/-}$ mice have previously been shown to have reduced *Svep1* mRNA expression in the lung and aorta (Winkler et al., 2020), and

have no gross phenotypic effects (Morooka et al., 2017; Winkler et al., 2020), were used for *ex vivo* analysis of vessel contraction.

Vessels from *Svep1*$^{+/-}$ mice showed a significantly higher contraction to U46619 (Fig. 5A&B) and PE (SF. 10A), compared to littermate controls. Incubation of vessels from C57BL/6J mice with an integrin α4 blocking antibody (10 µg ml^{-1}, MCA1230Ga, Fig. 5C), or an integrin α9 blocking antibody (10 µg ml^{-1}, 55A2C, Fig. 5D) significantly enhanced contraction to U46619. Simultaneous blocking of integrin α4β1 and α9β1 using blocking antibodies (Fig. 5E) or BOP (3 µM, Fig. 5F) caused a significant increase in vessel tension but did not enhance contraction compared to inhibition of individual integrins in isolation. Inhibition of integrin α4/α9 using BOP did not enhance contraction in *Svep1*$^{+/-}$ mice (Fig. 5G).

3.6 VGCCs and PKC regulate SVEP1-integrin α4/ α 9 inhibition of smooth muscle contraction

Aortas from C57BL/6J were either pre-incubated with BOP (Fig. 6A) or integrin α4 and α9 blocking antibodies (SF.10B) in the presence or absence of the VGCC inhibitor nifedipine (3 µM) prior to U46619 stimulation. VGCC inhibition significantly lowered both normal U46619-mediated vessel contraction (Fig. 6A), and the enhanced contraction caused by integrin α4/9 inhibition using BOP (Fig. 6A). In *Svep1*$^{+/-}$ mice, inhibition of VGCCs also significantly reduced U46619-mediated contraction (Fig. 6B). VGCCs activity is regulated by protein kinase C (PKC) (Ringvold & Khalil, 2017). Inhibition of PKC using bisindolylmaleimide I (BIM (I), 10 µM) significantly reduced normal U46619-mediated contraction (Fig. 6C), and the enhanced contraction caused by integrin α4/9 inhibition (Fig. 6C). BIM (I) inhibition of PKC also significantly reduced U46619-mediated contraction in *Svep1*$^{+/-}$ mice (Fig. 6D). These results show that SVEP1 regulation of GPCR-mediated contraction occurs through regulating PKC-mediated VGCC Ca^{2+} influx into the vessel.

To ensure the modulation in contractile responses elicited by SVEP1 and integrins α9β1/α4β1 is via receptor-mediated Ca^{2+} influx through VGCCs, and not a receptor-independent direct activation of VGCCs, we compared vessels stimulated with extracellular KCl between aortas from *Svep1*$^{+/-}$ mice and littermate controls (SF. 10 C) and aortas from C57BL/6J pre-incubated with BOP (SF. 10 D) stimulated with extracellular KCl. No alterations in contractile responses were detected between both

groups, confirming that SVEP1 did not directly affect VGCC activation and the observed alterations in U46619-mediated contraction is via receptor-mediated signalling.

3.7 ROCK regulates SVEP1 inhibition of smooth muscle contraction

In addition to regulating VGCC-PKC mediated Ca^{2+}-dependent vasoconstriction we investigated whether calcium sensitization mediated the regulation of VSMC contraction by SVEP1. ROCK signalling can inhibit MLCP activity to prolong MLC activity, maintaining VSMC contraction (Loirand & Pacaud, 2010). Pharmacological inhibition of ROCK (Y27632, 10 µM) significantly lowered both U46619-mediated control vessel contraction (Fig. 6E) and the enhanced contraction seen in *Svep1*$^{+/-}$ mouse aortas (Fig. 6E). SVEP1 reduces VSMC contraction by acting upon Ca^{2+}-dependent signalling and PKC to alter Ca^{2+} influx through VGCCs, and reduced calcium sensitivity via ROCK (Fig. 7).

4. Discussion

The data presented here represents the first investigation of SVEP1 and integrin α9β1 in vasoconstriction. SVEP1 was found to bind to integrin α9β1 and for the first time, the closely related integrin α4β1. Cell adhesion studies suggest that SVEP1 binds to integrin α4β1 through its CCP21 domain. Within the vasculature and in isolated VSMCs, we found expression of SVEP1, integrin α4β1, and α9β1 to be predominantly localised within the media layer confirming previous data (Jung et al., 2021). Due to the genetic association between *SVEP1* and *ITAG9* with BP, and the reported regulatory role for integrin α9β1 in airway contraction, we investigated whether SVEP1 could play a regulatory role in VSMC contraction via integrins α4β1/α9β1.

Our single cell $[Ca^{2+}]_i$ analysis showed that inhibition of SVEP1 or integrins α4/α9 caused an increase in $[Ca^{2+}]_i$ in response to several vasoconstrictors in iVSMC, suggesting a general regulatory effect upon receptor-mediated $[Ca^{2+}]_i$ elevation. Subsequent whole vessel studies where integrins α4/α9 were inhibited or SVEP1 levels were reduced in *Svep1*$^{+/-}$ mice, contractile force was also enhanced to either PE or U46619 application. SVEP1 or integrin α4/α9 inhibition had no effect on direct vessel contraction to smooth muscle depolarisation by KCl, indicating the regulatory role of SVEP1 is specific to receptor-mediated vasocontraction. We found similar increases in Ca^{2+} levels upon inhibition of integrin α4β1 or α9β1 and no additional

alterations in $[Ca^{2+}]_i$ were detected with co-inhibition of SVEP1 and the integrins in iVSMCs. Comparable results were observed in whole vessel contraction. These data suggest that the effect of SVEP1 on contraction is solely via integrin signalling and also indicates a level of redundancy between integrin α4β1 or α9β1 or a ceiling effect of SVEP1 inhibition upon vessel contraction. In the airway ligation of integrin α9β1 can prevent GPCR-mediated airway hyperresponsiveness (Chen et al., 2012), a phenotype comparable to the vascular role for integrin α9β1 and SVEP1 identified here. The physiology of airway smooth muscle cells is divergent from VSMCs, and integrin α9β1 instead regulates Ca^{2+} release from intracellular stores (Chen et al., 2012) meaning the downstream signalling events are likely to be different.

To determine the underlying SVEP1-integrin mediated regulation of GPCR-signalling we focused upon U46619 vasoconstriction mediated via the thromboxane A2 receptor (TXA_2R), that in addition to coupling with $G_{αq11}$, also couples with $G_{12/13}$ which activates ROCK, causing phosphorylation of MLCP and increased Ca^{2+} sensitivity in VSMCs (Pang, Guo, Su, Xie, Eto & Gong, 2005). Previous studies have uncovered various signalling pathways that control TXA_2R-mediated arteriole contraction, suggesting the relative importance of the pathways could be tissue/species specific. In bovine pulmonary arteries, contraction was mainly ROCK-mediated with little evidence of VGCC involvement (Alapati, McKenzie, Blair, Kenny, MacDonald & Shaw, 2007), whilst rat pulmonary artery contraction was PKC-VGCC mediated with little evidence of ROCK involvement (Cogolludo, Moreno, Bosca, Tamargo & Perez-Vizcaino, 2003). Rat caudal arteries found VGCCs and ROCK to induce contraction with little evidence of the requirement for PKC (Wilson, Susnjar, Kiss, Sutherland & Walsh, 2005). Mouse renal (Yan et al., 2019), mouse coronary (Jiang, Zhang, Yang, Zhou, Deng & Wu, 2021) and porcine coronary artery (Nobe & Paul, 2001) each found the Ca^{2+} sensitive VGCCs, ROCK, and PKC to all be required in U46619-mediated vasoconstriction.

In mouse aorta, we investigated both Ca^{2+}-dependent and Ca^{2+} sensitisation contractile mechanisms by inhibiting VGCCs and ROCK respectively, and additionally PKC, a central mediator of both mechanisms. Our data suggest that in the aorta U46619 initiates vessel contraction through both VGCC-mediated Ca^{2+}-dependent contraction and via ROCK kinase-mediated Ca^{2+}-sensitisation dependent contraction (Fig. 7) as described in other arterioles (Jiang, Zhang, Yang, Zhou, Deng & Wu, 2021; Nobe & Paul, 2001; Yan et al., 2019). Furthermore, comparable inhibition of U46619-

induced contraction in *Svep1*$^{+/-}$ mice or integrin α4β1/α9β1 inhibited mice to controls suggests that the vasoregulatory effect is mediated via the same pathway, indicating *Svep1* deficiency is mediated via PKC, VGCC and ROCK (Fig. 7). In these experiments we used HEPES buffered solution to bathe the vessels. It is conceivable that the environmental conditions used in myography could affect vessel responses to vasoconstrictor application, however we found our aortic contractile responses to be comparable with other studies stimulating aortic segments to U46619 when bathed in Krebs' buffer gassed continuously with 95% O_2 and 5% CO_2 (Heinze et al., 2014; Jimenez-Altayo et al., 2020).

Several studies have administered synthetic ligands to mimic important vasoactive ECM fragments which are otherwise un-exposed within the full-length ECM molecules (Davis, 2010). Dysregulation of the ECM is linked to several vascular-associated diseases including CAD (Galis & Khatri, 2002), heart failure (Westman et al., 2016), and stroke (Hill & Nemoto, 2015). SVEP1 is targeted by the protease ADAMTS-7 (Kessler et al., 2015), which also include genetic variants associated with CAD (Coronary Artery Disease Genetics, 2011; Nelson et al., 2017) and BP (Warren et al., 2017), and contains the linear peptide sequences Arg-Gly-Asp (RGD) and Leu-Asp-Val (LDV) sequences. Upon direct ligation to integrin αvβ3 (Mogford, Davis, Platts & Meininger, 1996; Wu, Mogford, Platts, Davis, Meininger & Davis, 1998) RGD inhibits VGCC current in smooth muscle, whilst the binding of LDV to integrin α4β1 (Waitkus-Edwards et al., 2002), α5β1 (Mogford, Davis & Meininger, 1997; Wu, Davis, Meininger, Wilson & Davis, 2001; Wu, Mogford, Platts, Davis, Meininger & Davis, 1998) and integrin α7β1 (Kwon et al., 2000) causes Ca^{2+} mediated smooth muscle contraction. It would be interesting to determine whether SVEP1 breakdown products also have altered vasoregulatory effects.

Recent studies produced conflicting data concerning *Svep1* deficiency in relation to the development of atherosclerotic plaques in mice (Jung et al., 2021; Winkler et al., 2020). Both investigations identified *SVEP1* expression in VSMCs and ECs within blood vessels but found opposing effects of SVEP1 in inflammatory cell recruitment, possibly highlighting distinct functions for SVEP1 in different cell-types, however, the cause for the phenotypic difference in atherosclerosis is unclear. In our data, *Svep1* deficiency increases contraction and would support SVEP1 as a protective molecule for reducing BP which might contribute to atheroprotection. Notably, human genetic

studies have identified associations between variants in both SVEP1 (Myocardial Infarction et al., 2016) and integrin α9β1 and BP (Evangelou et al., 2018; Levy et al., 2009). SVEP1, and integrins α4β1 and α9β1, as new mediators of GPCR-mediated vasoconstriction, provide a novel pathway whose activation could provide new therapeutic targets in vascular hypertension. Future studies should investigate whether the disease associated variants alter the contractile response of VSMCs and resistance vessels to contribute to an altered BP.

5. Conclusion

In conclusion we have described for the first time how the ECM protein SVEP1 lowers VSMC contractility via integrin α4β1 and/or α9β1 by influencing pathways that reduce Ca^{2+} influx through VGCCs and reduced calcium sensitivity, providing a new link between the extracellular environment and VSMC contraction.

Acknowledgements

We thank Professor Shigeyuki Kon at Fukuyama University for providing us with the anti-integrin α9 antibody (55A2C). We acknowledge the staff in the University of the Leicester Division of Biomedical Services for technical expertise and animal care. We thank the Advanced Imaging Facility (RRID:SCR_020967) at the University of Leicester for support.

Author Contribution Statement

G.E.M and T.R.W conceived the study and participated in the overall design, and coordination of the study. G.E.M designed and performed *in vitro* experiments. S.A.A performed the immunoprecipitation and cell binding studies. E.K and R.B.K performed IHC analysis. E.K and M.J.D performed wire myography experiments, with R.D.R and T.K providing support and supervision for the *ex vivo* models, and V. B providing statistical support. G.E.M, G.M, N.M.G, N.S, M.A.K, L.C, C.S, and T.R.W designed and generated the SVEP1 knockout iPSC lines. G.E.M., N.J.S. and T.R.W supervised the overall project. G.E.M and T.R.W wrote the manuscript. All authors reviewed the manuscript.

Source of Funding

The research presented here has received funding from the British Heart Foundation (BHF) (PG/20/10056 and SP16/4/32697) and was further supported by the BHF-DZHK VIAgenomics (SP/19/2/344612), the European Union Seventh Framework Programme FP7/2007-2013 under grant agreement number HEALTH-F2-2013-601456, and the van Geest Heart and Cardiovascular Diseases Research Fund, administered by the Department of Cardiovascular Sciences, University of Leicester.

Conflict of Interests

The authors declare no conflicting interests.

Declaration of Transparency and Scientific Rigour

This Declaration acknowledges that this paper adheres to the principles for transparent reporting and scientific rigour of preclinical research as stated in the *BJP* guidelines for Design & Analysis, Immunoblotting and Immunochemistry and Animal Experimentation, and as recommended by funding agencies, publishers and other organizations engaged with supporting research.

Data availability Statement

The data supporting the findings in this study are available from the corresponding author upon reasonable request.

References

Akamine R, Yamamoto T, Watanabe M, Yamazaki N, Kataoka M, Ishikawa M*, et al.* (2007). Usefulness of the 5' region of the cDNA encoding acidic ribosomal phosphoprotein P0 conserved among rats, mice, and humans as a standard probe for gene expression analysis in different tissues and animal species. J Biochem Biophys Methods 70**:** 481-486.

Alapati VR, McKenzie C, Blair A, Kenny D, MacDonald A, & Shaw AM (2007). Mechanisms of U46619- and 5-HT-induced contraction of bovine pulmonary arteries: role of chloride ions. British journal of pharmacology 151**:** 1224-1234.

Alexander SP, Christopoulos A, Davenport AP, Kelly E, Mathie A, Peters JA*, et al.* (2021a). THE CONCISE GUIDE TO PHARMACOLOGY 2021/22: G protein-coupled receptors. British journal of pharmacology 178 Suppl 1**:** S27-S156.

Alexander SP, Fabbro D, Kelly E, Mathie A, Peters JA, Veale EL*, et al.* (2021b). THE CONCISE GUIDE TO PHARMACOLOGY 2021/22: Catalytic receptors. British journal of pharmacology 178 Suppl 1**:** S264-S312.

Alexander SP, Fabbro D, Kelly E, Mathie A, Peters JA, Veale EL*, et al.* (2021c). THE CONCISE GUIDE TO PHARMACOLOGY 2021/22: Enzymes. British journal of pharmacology 178 Suppl 1**:** S313-S411.

Alexander SP, Kelly E, Mathie A, Peters JA, Veale EL, Armstrong JF*, et al.* (2021d). THE CONCISE GUIDE TO PHARMACOLOGY 2021/22: Introduction and Other Protein Targets. British journal of pharmacology 178 Suppl 1**:** S1-S26.

Alexander SP, Mathie A, Peters JA, Veale EL, Striessnig J, Kelly E*, et al.* (2021e). THE CONCISE GUIDE TO PHARMACOLOGY 2021/22: Ion channels. British journal of pharmacology 178 Suppl 1**:** S157-S245.

Alexander SPH, Roberts RE, Broughton BRS, Sobey CG, George CH, Stanford SC*, et al.* (2018). Goals and practicalities of immunoblotting and immunohistochemistry: A guide for submission to the British Journal of Pharmacology. British journal of pharmacology 175**:** 407-411.

Brozovich FV, Nicholson CJ, Degen CV, Gao YZ, Aggarwal M, & Morgan KG (2016). Mechanisms of Vascular Smooth Muscle Contraction and the Basis for Pharmacologic Treatment of Smooth Muscle Disorders. Pharmacol Rev 68**:** 476-532.

Chen C, Kudo M, Rutaganira F, Takano H, Lee C, Atakilit A*, et al.* (2012). Integrin alpha9beta1 in airway smooth muscle suppresses exaggerated airway narrowing. The Journal of clinical investigation 122**:** 2916-2927.

Cogolludo A, Moreno L, Bosca L, Tamargo J, & Perez-Vizcaino F (2003). Thromboxane A2-induced inhibition of voltage-gated K+ channels and pulmonary vasoconstriction: role of protein kinase Czeta. Circulation research 93**:** 656-663.

Coronary Artery Disease Genetics C (2011). A genome-wide association study in Europeans and South Asians identifies five new loci for coronary artery disease. Nature genetics 43**:** 339-344.

Curtis MJ, Alexander S, Cirino G, Docherty JR, George CH, Giembycz MA*, et al.* (2018). Experimental design and analysis and their reporting II: updated and simplified guidance for authors and peer reviewers. British journal of pharmacology 175**:** 987-993.

Davis GE (2010). Matricryptic sites control tissue injury responses in the cardiovascular system: relationships to pattern recognition receptor regulated events. Journal of molecular and cellular cardiology 48**:** 454-460.

Evangelou E, Warren HR, Mosen-Ansorena D, Mifsud B, Pazoki R, Gao H*, et al.* (2018). Genetic analysis of over 1 million people identifies 535 new loci associated with blood pressure traits. Nature genetics 50**:** 1412-1425.

Galis ZS, & Khatri JJ (2002). Matrix metalloproteinases in vascular remodeling and atherogenesis: the good, the bad, and the ugly. Circulation research 90**:** 251-262.

Gilges D, Vinit MA, Callebaut I, Coulombel L, Cacheux V, Romeo PH*, et al.* (2000). Polydom: a secreted protein with pentraxin, complement control protein, epidermal growth factor and von Willebrand factor A domains. The Biochemical journal 352 Pt 1**:** 49-59.

Halayko AJ, Salari H, Ma X, & Stephens NL (1996). Markers of airway smooth muscle cell phenotype. Am J Physiol 270**:** L1040-1051.

Heinze C, Seniuk A, Sokolov MV, Huebner AK, Klementowicz AE, Szijarto IA*, et al.* (2014). Disruption of vascular Ca2+-activated chloride currents lowers blood pressure. The Journal of clinical investigation 124**:** 675-686.

Hill JW, & Nemoto EM (2015). Matrix-derived inflammatory mediator N-acetyl proline-glycine-proline is neurotoxic and upregulated in brain after ischemic stroke. Journal of neuroinflammation 12**:** 214.

Ihara E, Hirano K, Hirano M, Nishimura J, Nawata H, & Kanaide H (2002). Mechanism of down-regulation of L-type Ca(2+) channel in the proliferating smooth muscle cells of rat aorta. J Cell Biochem 87**:** 242-251.

Jiang RS, Zhang L, Yang H, Zhou MY, Deng CY, & Wu W (2021). Signalling pathway of U46619-induced vascular smooth muscle contraction in mouse coronary artery. Clin Exp Pharmacol Physiol 48**:** 996-1006.

Jimenez-Altayo F, Ortiz-Romero P, Puertas-Umbert L, Dantas AP, Perez B, Vila E*, et al.* (2020). Stenosis coexists with compromised alpha1-adrenergic contractions in the ascending aorta of a mouse model of Williams-Beuren syndrome. Scientific reports 10**:** 889.

Jung IH, Elenbaas JS, Alisio A, Santana K, Young EP, Kang CJ*, et al.* (2021). SVEP1 is a human coronary artery disease locus that promotes atherosclerosis. Science translational medicine 13.

Karpanen T, Padberg Y, van de Pavert SA, Dierkes C, Morooka N, Peterson-Maduro J*, et al.* (2017). An Evolutionarily Conserved Role for Polydom/Svep1 During Lymphatic Vessel Formation. Circulation research 120**:** 1263-1275.

Kessler T, Zhang L, Liu Z, Yin X, Huang Y, Wang Y*, et al.* (2015). ADAMTS-7 inhibits re-endothelialization of injured arteries and promotes vascular remodeling through cleavage of thrombospondin-1. Circulation 131**:** 1191-1201.

Kwon MS, Park CS, Choi K, Ahnn J, Kim JI, Eom SH*, et al.* (2000). Calreticulin couples calcium release and calcium influx in integrin-mediated calcium signaling. Molecular biology of the cell 11**:** 1433-1443.

Levy D, Ehret GB, Rice K, Verwoert GC, Launer LJ, Dehghan A*, et al.* (2009). Genome-wide association study of blood pressure and hypertension. Nature genetics 41**:** 677-687.

Lilley E, Stanford SC, Kendall DE, Alexander SPH, Cirino G, Docherty JR*, et al.* (2020). ARRIVE 2.0 and the British Journal of Pharmacology: Updated guidance for 2020. British journal of pharmacology 177**:** 3611-3616.

Loirand G, & Pacaud P (2010). The role of Rho protein signaling in hypertension. Nature reviews Cardiology 7**:** 637-647.

Maguire EM, Xiao Q, & Xu Q (2017). Differentiation and Application of Induced Pluripotent Stem Cell-Derived Vascular Smooth Muscle Cells. Arteriosclerosis, thrombosis, and vascular biology 37**:** 2026-2037.

Mogford JE, Davis GE, & Meininger GA (1997). RGDN peptide interaction with endothelial alpha5beta1 integrin causes sustained endothelin-dependent vasoconstriction of rat skeletal muscle arterioles. The Journal of clinical investigation 100**:** 1647-1653.

Mogford JE, Davis GE, Platts SH, & Meininger GA (1996). Vascular smooth muscle alpha v beta 3 integrin mediates arteriolar vasodilation in response to RGD peptides. Circulation research 79**:** 821-826.

Morooka N, Futaki S, Sato-Nishiuchi R, Nishino M, Totani Y, Shimono C*, et al.* (2017). Polydom Is an Extracellular Matrix Protein Involved in Lymphatic Vessel Remodeling. Circulation research 120**:** 1276-1288.

Myocardial Infarction G, Investigators CAEC, Stitziel NO, Stirrups KE, Masca NG, Erdmann J*, et al.* (2016). Coding Variation in ANGPTL4, LPL, and SVEP1 and the Risk of Coronary Disease. The New England journal of medicine 374**:** 1134-1144.

Myocardial Infarction Genetics CECI (2016). Coding Variation in ANGPTL4, LPL, and SVEP1 and the Risk of Coronary Disease. New England Journal of Medicine 374**:** 1134-1144.

Nelson CP, Goel A, Butterworth AS, Kanoni S, Webb TR, Marouli E*, et al.* (2017). Association analyses based on false discovery rate implicate new loci for coronary artery disease. Nature genetics 49**:** 1385-1391.

Nelson MT, & Quayle JM (1995). Physiological roles and properties of potassium channels in arterial smooth muscle. Am J Physiol 268**:** C799-822.

Nobe K, & Paul RJ (2001). Distinct pathways of Ca(2+) sensitization in porcine coronary artery: effects of Rho-related kinase and protein kinase C inhibition on force and intracellular Ca(2+). Circulation research 88**:** 1283-1290.

Palmer EL, Ruegg C, Ferrando R, Pytela R, & Sheppard D (1993). Sequence and tissue distribution of the integrin alpha 9 subunit, a novel partner of beta 1 that is widely distributed in epithelia and muscle. The Journal of cell biology 123**:** 1289-1297.

Pang H, Guo Z, Su W, Xie Z, Eto M, & Gong MC (2005). RhoA-Rho kinase pathway mediates thrombin- and U-46619-induced phosphorylation of a myosin phosphatase inhibitor, CPI-17, in vascular smooth muscle cells. American journal of physiology Cell physiology 289**:** C352-360.

Pepinsky RB, Mumford RA, Chen LL, Leone D, Amo SE, Riper GV*, et al.* (2002). Comparative assessment of the ligand and metal ion binding properties of integrins alpha9beta1 and alpha4beta1. Biochemistry 41**:** 7125-7141.

Percie du Sert N, Hurst V, Ahluwalia A, Alam S, Avey MT, Baker M*, et al.* (2020). The ARRIVE guidelines 2.0: Updated guidelines for reporting animal research. British journal of pharmacology 177**:** 3617-3624.

Ringvold HC, & Khalil RA (2017). Protein Kinase C as Regulator of Vascular Smooth Muscle Function and Potential Target in Vascular Disorders. Adv Pharmacol 78**:** 203-301.

Samuelov L, Li Q, Bochner R, Najor NA, Albrecht L, Malchin N*, et al.* (2017). SVEP1 plays a crucial role in epidermal differentiation. Experimental dermatology 26**:** 423-430.

Sato-Nishiuchi R, Nakano I, Ozawa A, Sato Y, Takeichi M, Kiyozumi D*, et al.* (2012). Polydom/SVEP1 is a ligand for integrin alpha9beta1. The Journal of biological chemistry 287**:** 25615-25630.

Schindelin J, Arganda-Carreras I, Frise E, Kaynig V, Longair M, Pietzsch T*, et al.* (2012). Fiji: an open-source platform for biological-image analysis. Nature methods 9**:** 676-682.

Schwanzer-Pfeiffer D, Rossmanith E, Schildberger A, & Falkenhagen D (2010). Characterization of SVEP1, KIAA, and SRPX2 in an in vitro cell culture model of endotoxemia. Cellular immunology 263**:** 65-70.

Shur I, Socher R, Hameiri M, Fried A, & Benayahu D (2006). Molecular and cellular characterization of SEL-OB/SVEP1 in osteogenic cells in vivo and in vitro. Journal of cellular physiology 206**:** 420-427.

Touyz RM, Alves-Lopes R, Rios FJ, Camargo LL, Anagnostopoulou A, Arner A*, et al.* (2018). Vascular smooth muscle contraction in hypertension. Cardiovascular research 114**:** 529-539.

Waitkus-Edwards KR, Martinez-Lemus LA, Wu X, Trzeciakowski JP, Davis MJ, Davis GE*, et al.* (2002). alpha(4)beta(1) Integrin activation of L-type calcium channels in vascular smooth muscle causes arteriole vasoconstriction. Circulation research 90**:** 473-480.

Warren HR, Evangelou E, Cabrera CP, Gao H, Ren M, Mifsud B*, et al.* (2017). Genome-wide association analysis identifies novel blood pressure loci and offers biological insights into cardiovascular risk. Nature genetics 49**:** 403-415.

Webb RC (2003). Smooth muscle contraction and relaxation. Adv Physiol Educ 27**:** 201-206.

Westman PC, Lipinski MJ, Luger D, Waksman R, Bonow RO, Wu E*, et al.* (2016). Inflammation as a Driver of Adverse Left Ventricular Remodeling After Acute Myocardial Infarction. Journal of the American College of Cardiology 67**:** 2050-2060.

Widdop S, Daykin K, & Hall IP (1993). Expression of muscarinic M2 receptors in cultured human airway smooth muscle cells. American journal of respiratory cell and molecular biology 9**:** 541-546.

Wilson DP, Susnjar M, Kiss E, Sutherland C, & Walsh MP (2005). Thromboxane A2-induced contraction of rat caudal arterial smooth muscle involves activation of Ca2+ entry and Ca2+ sensitization: Rho-associated kinase-mediated phosphorylation of MYPT1 at Thr-855, but not Thr-697. The Biochemical journal 389**:** 763-774.

Winkler MJ, Muller P, Sharifi AM, Wobst J, Winter H, Mokry M*, et al.* (2020). Functional investigation of the coronary artery disease gene SVEP1. Basic Res Cardiol 115**:** 67.

Wu X, Davis GE, Meininger GA, Wilson E, & Davis MJ (2001). Regulation of the L-type calcium channel by alpha 5beta 1 integrin requires signaling between focal adhesion proteins. The Journal of biological chemistry 276**:** 30285-30292.

Wu X, Mogford JE, Platts SH, Davis GE, Meininger GA, & Davis MJ (1998). Modulation of calcium current in arteriolar smooth muscle by alphav beta3 and alpha5 beta1 integrin ligands. The Journal of cell biology 143**:** 241-252.

Yan H, Zhang MZ, Wong G, Liu L, Kwok YSS, Kuang SJ*, et al.* (2019). Mechanisms of U46619-induced contraction in mouse intrarenal artery. Clin Exp Pharmacol Physiol 46**:** 643-651.

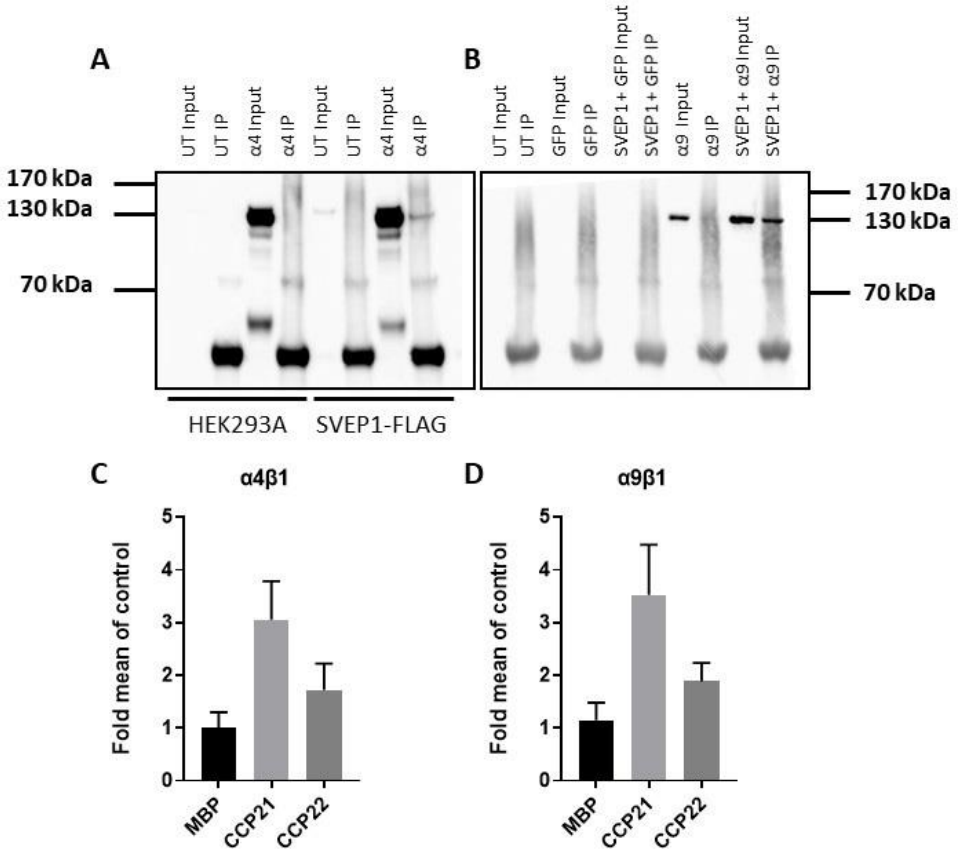

Figure 1: Integrin α4β1 and α9β1 bind to SVEP1 Immunoblots with anti-α4 (A) and anti-GFP (B) antibodies following immunoprecipitation of protein lysates using anti-FLAG agarose from HEK293A or HEK293A cells stably overexpressing SVEP1-FLAG transfected with integrin α4β1 (α4) or HEK293A cells co-transfected with GFP only control, or GFP-integrin α9β1 (α9) and SVEP1-FLAG plasmids. Binding efficiency of HEK293A cells stably overexpressing integrin α4β1 (C) or α9β1 (D) to surface coated with 100 nM mannose binding protein (MBP), or SVEP1 21st or 22nd CCP domain (±SD, n=3). Data is normalised to MBP control to account for variation in cell binding between experiments.

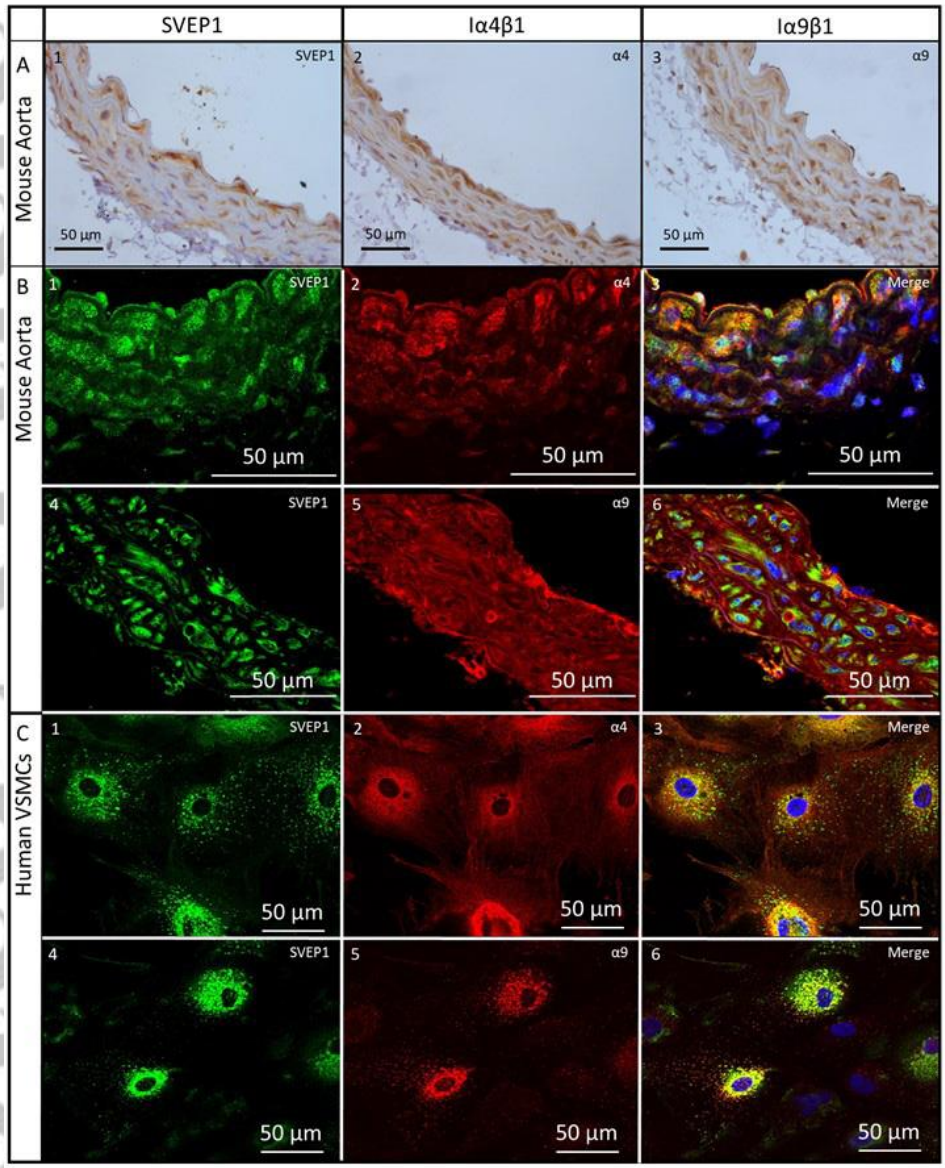

Figure 2: SVEP1, integrin α4β1 and integrin α9β1 expression in vascular smooth muscle. (A) Immunohistochemical staining of SVEP1 (1), integrin α4β1 (2), and integrin α9β1 (3) in mouse aorta sections. (B) Dual fluorescent staining of SVEP1 (1 & 3) and integrin α4β1 (2 & 3), and SVEP1 (4 & 6) and integrin α9β1 (5 & 6) in mouse aorta sections. (C) Dual fluorescent staining of SVEP1 (1 & 3) and integrin α4β1 (2 & 3), and SVEP1 (4 & 6) and integrin α9β1 (3 & 4) in human vascular smooth muscle cells.

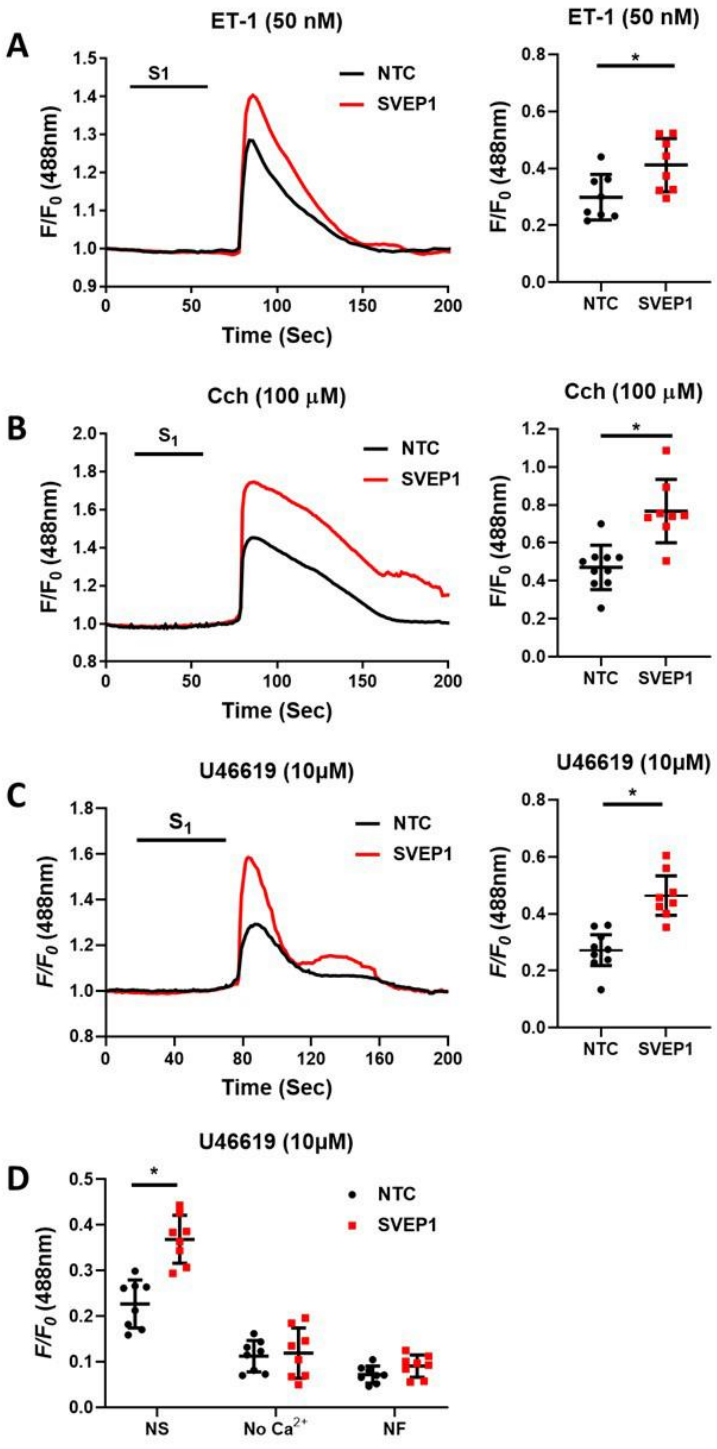

Figure 3: SVEP1 inhibition increases iVSMC [Ca2+]i to several vasoconstrictors iVSMCs were treated with either non-targeting control (NTC), or SVEP1 siRNA for 48 hrs prior to Fluo3 loading and vasoconstrictor challenge for 45 secs (S1). (A) Mean trace and maximal fluorescence signal (dot plot, F/F0) are shown for ET-1 (50 nM, n=8), (B) Cch (100 μM, NTC n=10, SVEP1 n=8), and (C) U46619 (10 μM, n=8). (D) Imaging buffer was changed to a zero Ca2+ buffer (No Ca2+) for 2 mins, or incubated in nifedipine (3 μM) for 30 mins prior to U46619 challenge (10 μM, n=8). Data are represented as mean±SD. * $P < 0.05$, unpaired t-test.

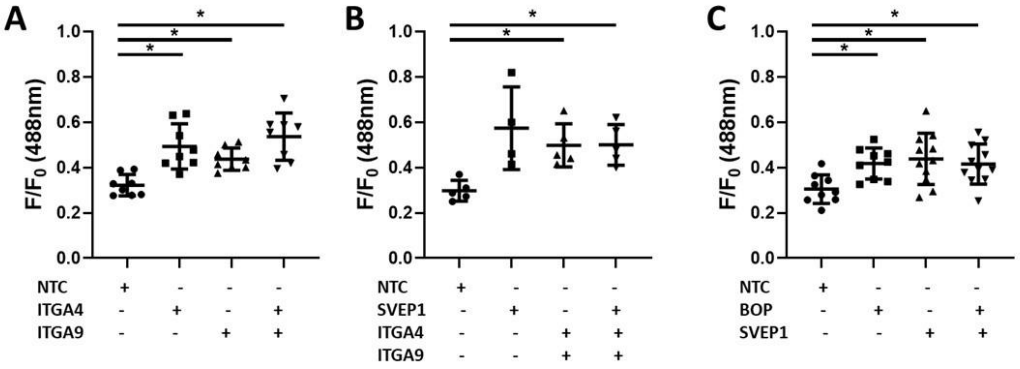

Figure 4: Simultaneous inhibition of SVEP1 and integrin α4 or α9 does not induce additional [Ca2+]i elevation in iVSMCs iVSMCs were treated with non-targeting control (NTC), ITGA4, ITGA9 or SVEP1 siRNA for 48 hrs, or the dual integrin α4β1-α9β1 inhibitor BOP for 2 hrs prior to Fluo3 loading and ET-1 (50 nM) challenge for 45 secs. Maximal fluorescence signal (F/F0) are shown (A) n=8, B) NTC, ITGA4, ITGA9 n=5, SVEP1 n=4, C) NTC, BOP n=9, SVEP1 n=10, SVEP1 & BOP n=11). Data are represented as mean±SD. * $P < 0.05$, one-way ANOVA followed by Tukey's post hoc test.

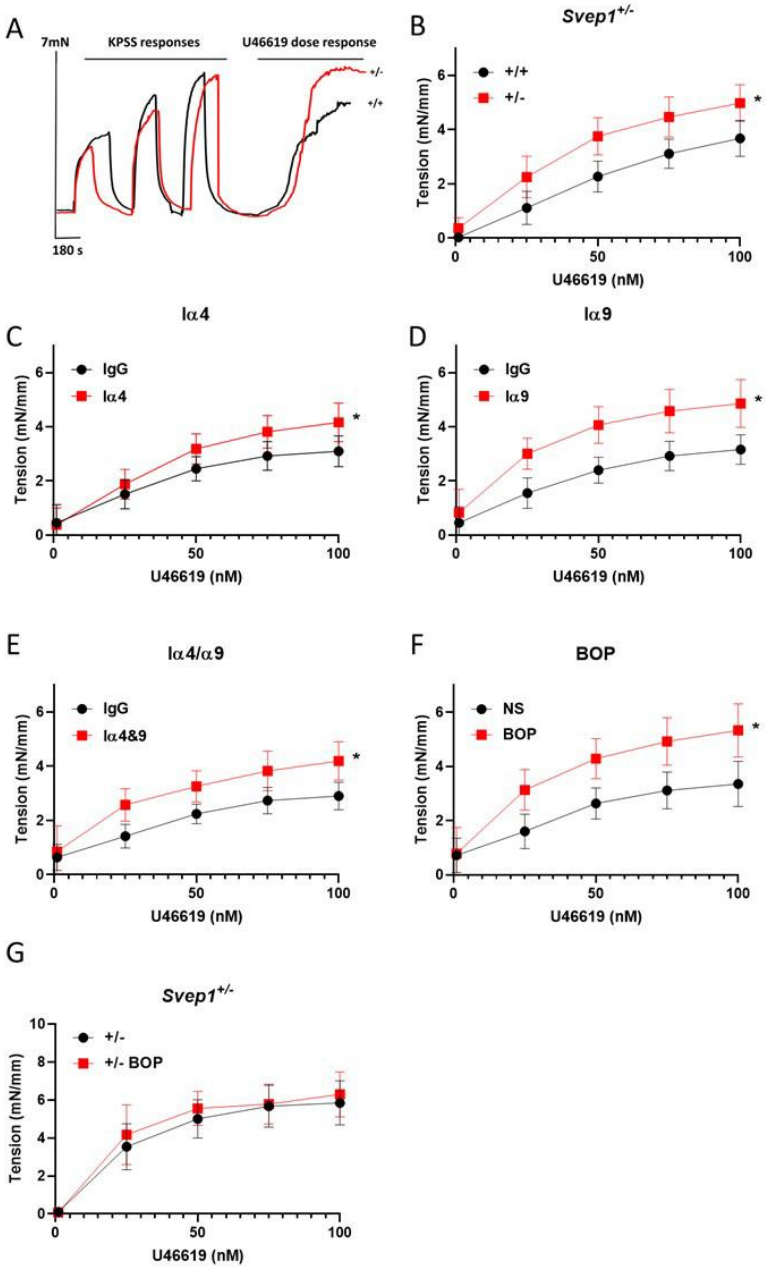

Figure 5. SVEP1 or integrin α4/9 inhibition enhances blood vessel contraction (A) Example traces showing force generation of aortas from Svep1+/- (+/-, red trace) and littermate control (+/+, black trace) mice stimulated with U46619. (B) Aortas from Svep1+/- mice were stimulated with U46619 (+/+ n=11, +/- n=13) and force generation was recorded by wire myography. (C) Aortas from C57BL/6J mice were incubated overnight with an integrin α4 (10 μg/ml) (IgG n=10, ITGA4 n=10), (D) integrin α9 (10 μg/ml) (IgG n=10, ITGA9 n=10), (E) a combination of both integrin α4 & α9 blocking antibodies (IgG n=11, 4&9 n=12), or (F) the dual integrin α4 and α9 inhibitor BOP (3 μM) (NS n=6, BOP=10) prior to U46619 application. (G) Aortas from Svep1+/- mice were incubated overnight with BOP (+/- n=10, +/- BOP n=10) and force generation was recorded. Data are represented as mean values, bar represents 95% confidence intervals, * $P < 0.05$, mixed-effect models.

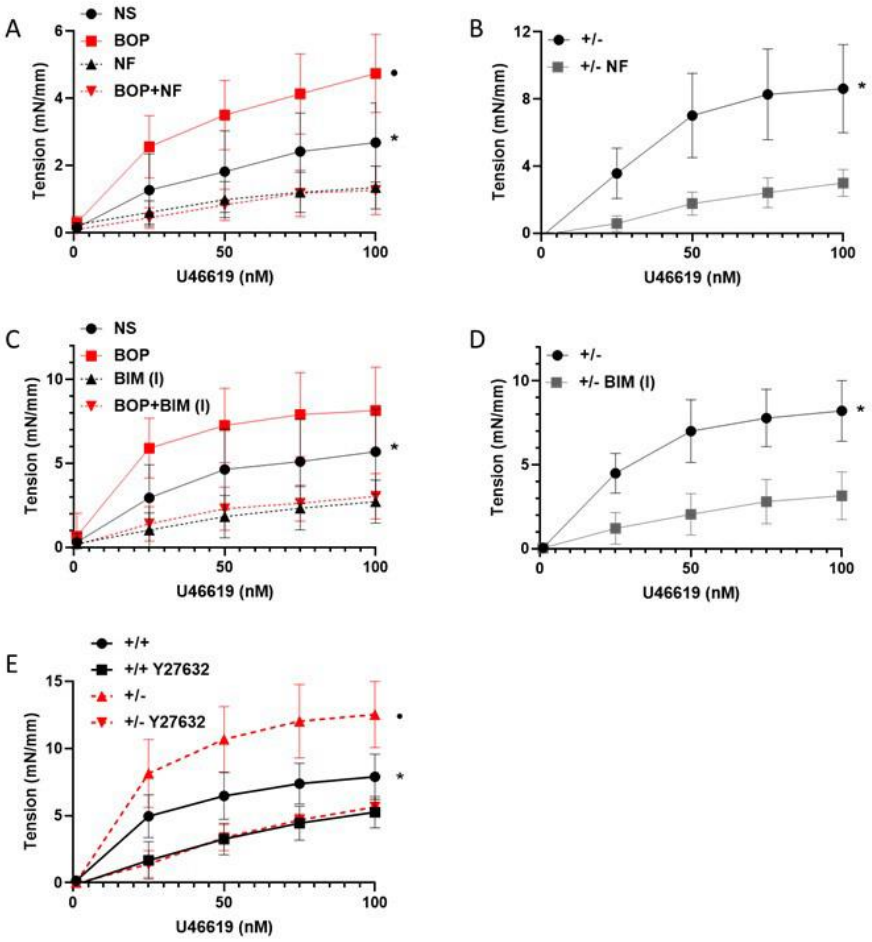

Figure 6: Integrin α4/9 regulates blood vessel contraction via Ca2+ influx through VGCCs in a PKC and ROCK dependent manner (A) Aortas from C57BL/6J mice were incubated with the dual integrin α4/9 inhibitor BOP overnight and incubated with the VGCC blocker nifedipine (NF) for 30 mins prior to U46619 application and force generation was recorded (n=7, * $P < 0.05$ NS vs. NF, • $P < 0.05$ BOP vs. BOP+NF). (B) Aortas from Svep1+/- mice were incubated with NF (n=6, * $P < 0.05$). (C) Aortas from C57BL/6J mice were incubated BOP overnight and incubated with the PKC inhibitor BIM (I) for 30 mins prior to U46619 application (n=7, * $P < 0.05$, NS vs. BIM (I), • $P < 0.05$ BOP vs. BOP+BIM (I)). (D) Aortas from Svep1+/- mice were incubated with BIM (I) (n=9, * $P < 0.05$). (E) Aortas from Svep1+/- mice (+/-) or littermate control mice (+/+) were incubated with the ROCK inhibitor Y27632 for 30 mins prior to U46619 application and force generation was recorded (n=7, * $P < 0.05$ +/+ vs. +/+ Y2673, • $P < 0.05$ +/- vs. +/- Y2673). Data are represented as mean values, bar represent 95% confidence intervals; p-values derived from mixed-effect models.

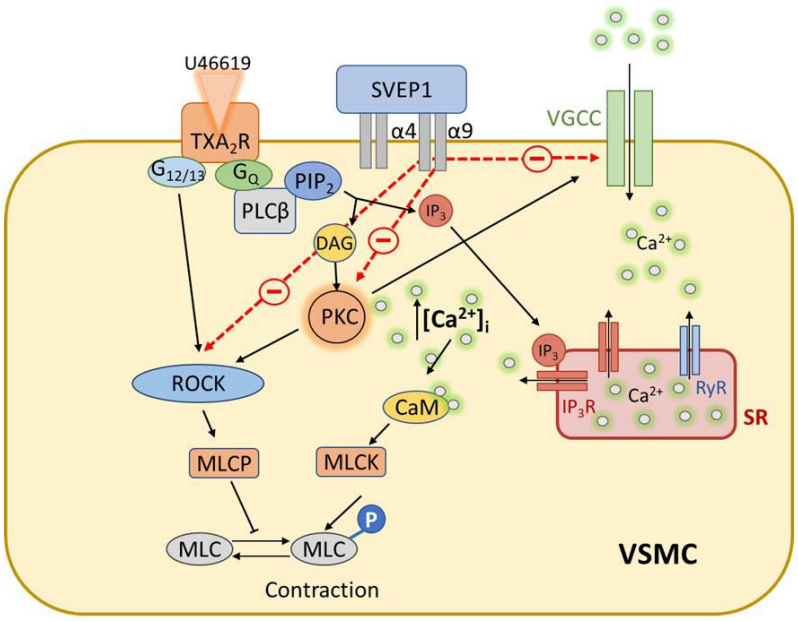

Figure 7: Schematic for proposed model of how SVEP1 regulated GPCR-mediated vasoconstriction U46619 binds to TAX2R to activate Gαq and G12/13 signalling. Gαq activates PLCβ which hydrolyses PIP2 into DAG and IP3. Binding of IP3 to the IP3 receptors on the SR induces Ca2+ release from stores. DAGactivated PKC promotes the opening of VGCCs to initiate Ca2+ influx into the cell. Ca2+ -bound CaM activates MLCK which phosphorylates MLC leading to contraction. Activation of PKC and G12/13 also activates ROCK which inhibits MLCP promoting further activation of MLC and contraction. SVEP1 regulates contractility of VSMC via integrins α4/α9 by interacting with both calcium-dependent pathways that reduce PKC activity and the influx of extracellular Ca2+ through VGCCs, and calcium sensitisation via ROCK. Abbreviations: α4, integrin α4β1, α9, integrin α9β1, CaM, calmodulin, DAG, diacylglycerol, IP3, inositol triphosphate, MLC(K)(P), myosin light chain (kinase)(phosphatase), PIP2 , phosphatidylinositol diphosphate, PKC, protein kinase C, PLCβ, phospholipase C β, ROCK Rho A/Rho kinase, SR, sarcoplamic reticulum, TXA2R, thromboxane A2 receptor, VGCCs, voltage gated calcium channels, VSMC, vascular smooth muscle cell.

Graphical Abstract